Phonon Laser Action in a Tunable Two-Level System

Ivan S. Grudinin, Hansuek Lee, O. Painter, and Kerry J. Vahala*

Department of Applied Physics, California Institute of Technology, 1200 East California Boulevard, Pasadena, California 91125, USA

(Received 15 July 2009; revised manuscript received 2 December 2009; published 22 February 2010)

The phonon analog of an optical laser has long been a subject of interest. We demonstrate a compound microcavity system, coupled to a radio-frequency mechanical mode, that operates in close analogy to a two-level laser system. An inversion produces gain, causing phonon laser action above a pump power threshold of around 7 μW. The device features a continuously tunable gain spectrum to selectively amplify mechanical modes from radio frequency to microwave rates. Viewed as a Brillouin process, the system accesses a regime in which the phonon plays what has traditionally been the role of the Stokes wave. For this reason, it should also be possible to controllably switch between phonon and photon laser regimes. Cooling of the mechanical mode is also possible.

DOI: 10.1103/PhysRevLett.104.083901 PACS numbers: 42.60.Da, 42.55.−f, 71.36.+c

Introduction.—The possibility of phonon laser action has been proposed in a wide range of physical systems including paramagnetic ions in a lattice [1], paraelectric crystals [2], isolated trapped ions [3], semiconductors [4,5], nanomechanics [6], nanomagnets [7], and others [8]. Observations of phonon stimulated emission have been reported in cryogenic $Al_2O_3:Cr^{3+}$ [9–11] and $Al_2O_3:V^{4+}$ [12], and in semiconductor superlattices [13] (see also references within [11]). However, only recently has phonon laser action been reported using a harmonically bound magnesium ion [14]. Here, using a compound microcavity system, a phonon laser that operates in close analogy to a two-level laser system is demonstrated. The approach uses intermodal coupling induced by radiation pressure [15] and can also provide a spectrally selective means to detect phonons. Moreover, there is currently great interest in optomechanical cooling [16], and evidence of intermodal cooling is observed.

Compound microcavity systems are sometimes called photonic molecules [17–19], and herein this is a particularly apt interpretation. Hybridized orbitals of an electronic system are replaced by optical supermodes of the compound (photonic molecule) system, and transitions between their corresponding energy levels are induced by a phonon field. For conditions very typical of the optical microresonators studied here, it behaves as a two-level laser system, but with a peculiar twist: the traditional roles of the material (laser medium) and cavity modes (lasing field) are reversed. Instead, the medium is now purely optical, while the laser field is provided by the material as a phonon mode.

Compound microcavity systems provide beneficial spectral controls that impact both phonon laser action and cooling, not least of which are finely spaced optical levels whose transition energies are commensurate with phonon energies. Significantly, these level spacings are continuously tunable by adjustment of optical coupling. Amplification and cooling thus occur around a tunable line center, in contrast with cavity optomechanical phenomena demonstrated to date [16]. Moreover, the creation of these finely spaced levels does not require increasing the microcavity dimensions and hence has a minimal effect on the optomechanical interaction strength. Also, cooling with nearly ideal Stokes suppression and high pump coupling is possible. Other features are discussed below.

System and model.—A schematic and micrographs of the optomechanical system are provided in Fig. 1. It features two microtoroid whispering-gallery-mode (WGM) resonators [20]. Although each resonator supports many optical modes, only two modes (one from each microtoroid) contribute to the physical system. These modes can be made degenerate in frequency by thermal control of the microtoroids. To couple and outcouple optical power, a tapered optical fiber is used as shown in Fig. 1 [21,22].

Evanescent coupling of the initially uncoupled whispering-gallery modes is possible through control of the air gap between the microtoroids. This produces two

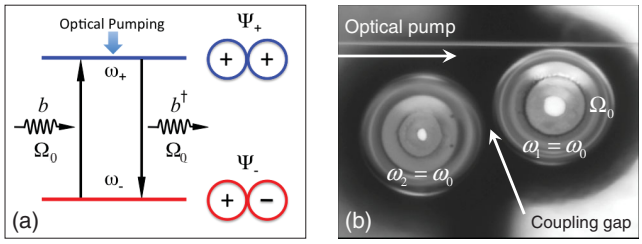

FIG. 1 (color). (a) Two-level phonon laser energy level diagram including schematics of the photonic molecule symmetric and antisymmetric orbitals. (b) Physical implementation of the phonon laser using coupled microtoroids. Optical excitation and observation are enabled by a tapered fiber coupler that is visible in the image. The microtoroids are approximately 63 μm in diameter: the left toroid is fabricated using a 4 μm silica layer and has an approximately 12.5 μm minor diameter, while the right toroid is fabricated using a 2 μm silica layer and has an approximately 8.7 μm minor diameter.

new normal modes (supermodes) that, for initially degenerate uncoupled modes, are symmetric and antisymmetric combinations of the uncoupled modes. Their respective eigenfrequencies are split by an amount that depends exponentially upon the air gap [23]. Modal spectra at several different air gaps are presented in Fig. 2. These were obtained by monitoring the transmission through the fiber taper as an excitation laser is scanned in the frequency vicinity of the optical resonances. The measured supermode splitting as a function of the air gap is also plotted to verify the exponential dependence. Control of splitting frequency from 10 MHz to nearly 10 GHz is demonstrated in Fig. 2. Larger splittings are possible using smaller radii microtoroids so as to enhance the evanescent coupling strength. An alternative viewpoint of this coupling process is as an avoided crossing. By thermal control, a microtoroid resonance at ω_1 can be scanned so as to cross a resonance (ω_2) in the other microtoroid. The normal mode splitting during such frequency scan appears as an avoided crossing, an example of which is also provided in Fig. 2. At higher coupled powers, observation of the full spectrum was complicated by thermal nonlinearity. Additional spectral modeling and observations of the thermal nonlinearity are provided in Ref. [24]. The nonlinearity primarily impacts pumping of the red supermode.

The Hamiltonian for optomechanical interaction in a multimode optical cavity has been considered elsewhere

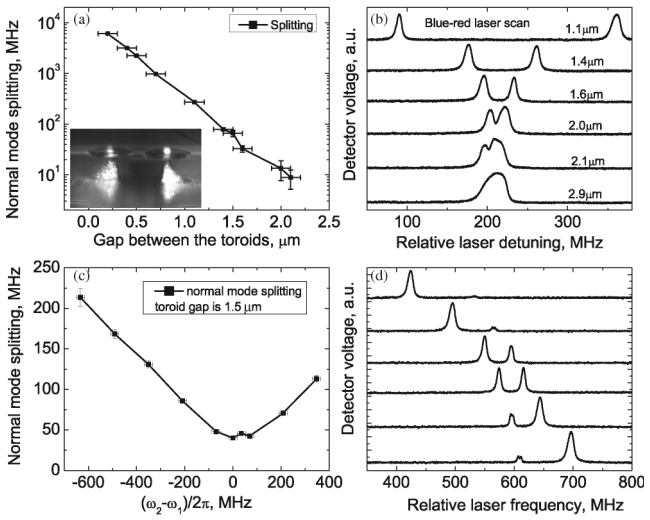

FIG. 2. Controllable splitting of the supermodes in coupled microtoroids with major diameters of 66 and 69 μm is presented in panels (a) and (b). A measured set of optical spectra taken over a range of coupling gaps appears in (b), while the measured splitting frequencies as a function of gap distance are plotted in (a). The inset provides a side view of the coupled microtoroid system. Avoided crossing of the optical modes is presented in panels (c) and (d). Here, the temperature of one microtoroid was gradually changed to adjust the WGM frequency. Measured spectra are presented in (d), and the avoided crossing as a function of frequency tuning is given in (c).

[15,25]. Extension to the present system of coupled microtoroids in which one microtoroid contains a mechanical mode (frequency Ω_0 and effective mass m_{eff}) yields

$$H = \hbar\omega_+ \Psi_+^\dagger \Psi_+ + \hbar\omega_- \Psi_-^\dagger \Psi_- + \hbar\Omega_0 b^\dagger b + \frac{\hbar g x_0}{2}(b\Psi_+^\dagger \Psi_- + \Psi_-^\dagger \Psi_+ b^\dagger), \quad (1)$$

where ω_+ and ω_- are the optical frequencies of the supermodes (the underlying uncoupled resonances are assumed degenerate with frequency ω_0), $g = \omega_0/R$ is the optomechanical coupling coefficient (R is radius of the microtoroid that contains the mechanical mode), $x_0 = \sqrt{\hbar/2m_{\text{eff}}\Omega_0}$, while Ψ_-, Ψ_+, and b are the lowering operators for the supermodes (defined to be red and blue, respectively) and the mechanical mode. In deriving this Hamiltonian, the energy nonconserving terms as well as the conventional optomechanical terms (i.e., single mode coupling) have been omitted. The first interaction term in this Hamiltonian describes the destruction of one phonon and promotion of a photon from the red supermode into the blue supermode, while the second term (adjoint) describes the reverse process. The Heisenberg equations of motion for the mechanical mode and the operator $p \equiv \Psi_-^\dagger \Psi_+$ (with damping added) are

$$\dot{b} = \left[-\imath\Omega_0 - \frac{\Gamma}{2}\right] b - \imath\frac{\Omega_R}{2} p + f(t), \quad (2)$$

$$\dot{p} = \left[-\imath\Delta\omega - \frac{\gamma}{2}\right] p - \imath\frac{\Omega_R}{2}\Delta N b + F(t), \quad (3)$$

where $\Delta\omega \equiv \omega_+ - \omega_-$; $\Delta N \equiv \Psi_+^\dagger \Psi_+ - \Psi_-^\dagger \Psi_-$; $\Omega_R \equiv g x_0$; Γ is the intrinsic energy decay rate of the mechanical mode; $2\gamma = \gamma_1 + \gamma_2$, where $\gamma_{1,2}$ are the optical decay rates of the WGMs of each toroid; and $f(t)$, $F(t)$ are Langevin operators, included here only for completeness. The structure of these equations is equivalent to corresponding equations for a two-level laser wherein p is identified with the polarization of the transition, ΔN is the optical (as opposed to electronic) inversion operator, and γ is the polarization dephasing rate (equivalently, T_2^{-1}). To find the mechanical gain, they can be solved in the regime of weak coupling in which the optical cavity decay rate (effectively, the polarization dephasing rate) exceeds the mechanical dissipation rate (i.e., $\gamma \gg \Gamma$),

$$G = \left(\frac{\Omega_R}{2}\right)^2 \frac{\Delta N \gamma}{(\Delta\omega - \Omega_0)^2 + (\frac{\gamma}{2})^2}. \quad (4)$$

In addition to being proportional to the inversion ΔN, the gain has a spectral shape that is Lorentzian with linewidth γ. Significantly, the gain spectrum line center, i.e., $\Delta\omega = \Omega_0$, can be controlled through adjustment of $\Delta\omega$ as illustrated in Fig. 2. Setting $\Gamma = G$, the threshold condition, gives the threshold pump power for the phonon laser as

$P_{cT} \approx N_+ \gamma \hbar \omega_+ = \Gamma \gamma^2 \hbar \omega_+ / \Omega_R^2$ (for blue-supermode threshold density of N_+ at line center).

At a fundamental level, the scattering of the blue-supermode pump photon resembles stimulated-Brillouin scattering [15]. Even more generally, it is similar in form to parametric down-conversion, wherein the less strongly damped field in a parametrically partnered pair will experience stimulated emission and amplification [26]. In contrast to prior Brillouin or Raman systems that are typically restricted to the stimulated photon branch, the present system provides access to both phonon ($\gamma \gg \Gamma$ regime of this Letter) and photon ($\gamma \ll \Gamma$) stimulated regimes. Indeed, this possibility was recognized in early studies of stimulated-Brillouin scattering wherein a traveling-wave geometry was interpreted as a phonon amplifier [27]. The conditions there (and typical of Brillouin scattering in the traveling-wave geometry), however, feature stronger spatial damping of the phonons compared to the photons and therefore make clear that optical amplification was observed [26]. Lower temperature operation could alter this balance [26]. The delineation of the parametric instability [15] into these phonon and photon stimulated regimes has not previously been noted but is nonetheless important to microdevice applications. Such features as the operative degree of freedom (optical or mechanical), fluctuations, coherence of motion, and gain bandwidth, to name a few, are significantly impacted by the regime.

Phonon laser operation.—A fiber laser from KOHERAS A/S with a kilohertz-range linewidth at a wavelength of 1550 nm served as the optical pump. The power transmitted through the tapered fiber coupler was detected with amplified New Focus detectors 1611 and 1817. To monitor coherent mechanical motion of the system, corresponding spectral components in the detected photocurrent are monitored on an electrical spectrum analyzer. Such components show a pronounced increase in magnitude when the threshold condition is achieved.

Tuning of the mechanical gain spectrum to selectively pull modes from the noise is illustrated in Fig. 3(c). Each scan in this plot is taken with the air gap at a different setting so as to vary the supermode splitting and hence the mechanical gain spectrum line center. The overall scan frequency range is 40–400 MHz. The "bump" appearing at higher frequencies in the upper scan is the result of amplification. It is progressively tuned to lower frequencies by increase of the air-gap separation. Several mechanical modes are amplified as the gain maximum comes into their spectral vicinity. Gain tuning control to produce phonon laser action is illustrated in Figs. 3(a) and 3(b), wherein the mechanical gain line center was adjusted to coincide with mechanical modes at 21.5 MHz and at 41 MHz, and pumping was sufficient to induce selective phonon laser action. All measured mechanical modes belong to the toroid nearest the fiber taper.

Plot of the rf signal power versus optical pump power confirms laser threshold behavior (Fig. 4). Using $m_{\text{eff}} = 5 \times 10^{-11}$ kg [28], $\Gamma = \Omega/Q_{\text{mech}} = 2\pi \times (23.4\ \text{MHz})/10^3 = 2.5 \times 10^5$ (estimated from mechanical spectral measurement), and $Q = 4 \times 10^7$ (from optical spectral measurement) in the threshold equation gives an oscillation threshold of 6 μW, in reasonable agreement with the data.

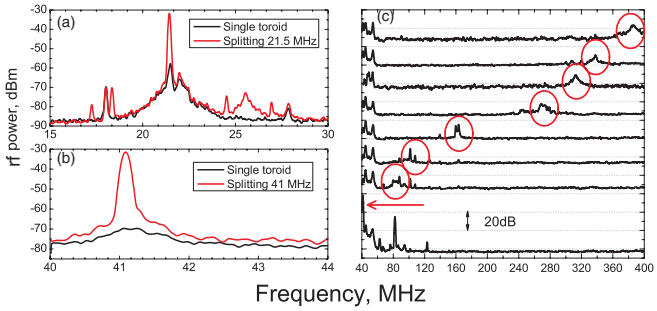

FIG. 3 (color). (a), (b) Spectrum analyzer traces of the detected photocurrent. Phonon lasing spectra of two mechanical modes are shown in red. The spectrum (a) corresponds to a transition frequency (i.e., supermode splitting) of 21.5 MHz, while the spectrum (b) corresponds to a transition frequency of 41 MHz. The spectra shown in black are taken for the same optical pumping powers but with the resonators uncoupled, thereby destroying the transition. (c) Observation of amplified spectra for subthreshold pumping at a series of transition frequencies. The gain causes a spectral bump to appear on account of amplified mechanical modes. The spectral location of the gain maximum is determined by the transition frequency (as controlled by the gap). The transition frequency is varied from 40 MHz (lower trace) to nearly 400 MHz (upper trace). For some frequencies, the gain maximum coincides with mechanical resonances, which are subsequently "pulled" from the noise.

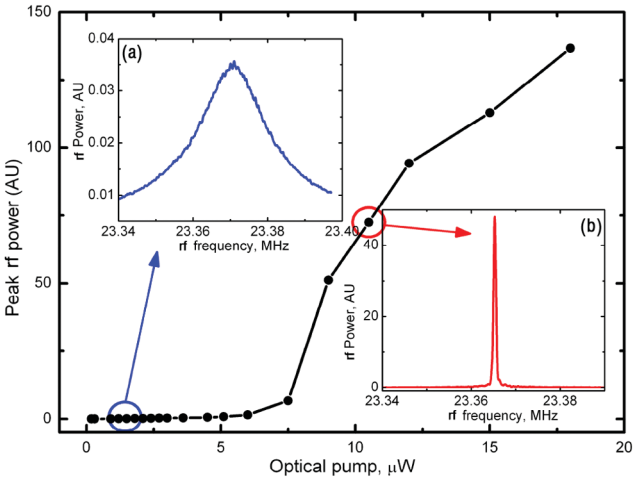

FIG. 4 (color). Plot of rf photocurrent power versus coupled optical pump power for a mechanical mode at 23.4 MHz. A clear threshold is observable in the data. Insets of the measured mechanical line shape function at the indicated pumping points below (a) and above (b) threshold show line narrowing. The below-threshold spectrum in (a) has been magnified 800 × .

Red-supermode pumping [negative inversion in Eq. (4)] will produce damping of the mechanical mode and optomechanical cooling through absorption of mechanical quanta. Despite power limitations imposed by the thermal nonlinearity, evidence of cooling was observed as a decrease in the absolute power level of mechanical spectral peaks with increasing optical power. The range, however, was limited due to the thermal nonlinearity.

Summary.—A tunable phonon amplifier and phonon laser have been demonstrated that operate in close analogy to a two-level optical laser system. A compound whispering-gallery resonator (photonic molecule) is used to create finely spaced levels with transition frequencies commensurate to phonon frequencies and without sacrificing cavity size or optomechanical coupling strength (i.e., g parameter). Continuous wideband tuning of the level separation—and hence the gain (and cooling) band—is possible by adjustment of resonator coupling. Also, a photon (as opposed to phonon) laser regime has been described. Extension to multilevel systems using multiple coupled resonators is possible. Evidence of mechanical cooling has been observed by excitation of the red supermode, and the two-level system enables ideal Stokes wave suppression with excellent pump coupling. Cavities are sensitive transducers for detection of weak displacements and forces [29], and an optomechanical compound system such as described here may also have application for improved readout and quantum backaction enhancement [30]. Moreover, the relation of the present work to observations of the parametric instability [28] of cavity optomechanics [16] will be detailed elsewhere. The present cavity design also enables spectrally selective and tunable detection of phonons through absorption (red pump) by the two-level system. Analysis of the response shows that thermal phonons set a background detection level for this process. Efficient detection of phonons also requires operation in the regime for which optical damping is more rapid than mechanical damping. Finally, while the embodiment described here requires additional coupling structures to link it to a phonon source, the use of optomechanical crystal based devices would enable integration of both phonon sources, detectors, and vibrational waveguides [31]. This approach would also enable the coupling of the localized phonon laser mode to extended modes of a solid in complete analogy to an optical laser.

This work was supported by DARPA.

*vahala@caltech.edu

[1] C. Kittel, Phys. Rev. Lett. **6**, 449 (1961).
[2] L. A. Vredevoe and I. F. Silvera, Solid State Commun. **8**, 1715 (1970).
[3] S. Wallentowitz, W. Vogel, I. Siemers, and P. E. Toschek, Phys. Rev. A **54**, 943 (1996).
[4] I. Camps, S. S. Makler, H. M. Pastawski, and L. E. F. F. Torres, Phys. Rev. B **64**, 125311 (2001).
[5] H. C. Liu, C. Y. Song, Z. R. Wasilewski, A. J. SpringThorpe, J. C. Cao, C. Dharma-Wardana, G. C. Aers, D. J. Lockwood, and J. A. Gupta, Phys. Rev. Lett. **90**, 077402 (2003).
[6] I. Bargatin and M. L. Roukes, Phys. Rev. Lett. **91**, 138302 (2003).
[7] E. M. Chudnovsky and D. A. Garanin, Phys. Rev. Lett. **93**, 257205 (2004).
[8] J. Chen and J. B. Khurgin, IEEE J. Quantum Electron. **39**, 600 (2003).
[9] E. B. Tucker, Phys. Rev. Lett. **6**, 547 (1961).
[10] P. Hu, Phys. Rev. Lett. **44**, 417 (1980).
[11] P. A. Fokker, J. I. Dijkhuis, and H. W. deWijn, Phys. Rev. B **55**, 2925 (1997).
[12] W. E. Bron and W. Grill, Phys. Rev. Lett. **40**, 1459 (1978).
[13] A. J. Kent, R. N. Kini, N. M. Stanton, M. Henini, B. A. Glavin, V. A. Kochelap, and T. L. Linnik, Phys. Rev. Lett. **96**, 215504 (2006).
[14] K. Vahala, M. Hermann, S. Knünz, V. Batteiger, G. Saathoff, T. W. Hänsch, and T. Udem, Nature Phys. **5**, 682 (2009).
[15] V. B. Braginsky, S. E. Strygin, and S. P. Vyatchanin, Phys. Lett. A **287**, 331 (2001).
[16] T. J. Kippenberg and K. J. Vahala, Science **321**, 1172 (2008).
[17] M. Bayer, T. Gutbrod, J. P. Reithmaier, A. Forchel, T. L. Reinecke, P. A. Knipp, A. A. Dremin, and V. D Kulakovskii, Phys. Rev. Lett. **81**, 2582 (1998).
[18] D. Barnes, S. M. Mahurin, A. Mehta, B. G. Sumpter, and D. W. Noid, Phys. Rev. Lett. **88**, 015508 (2001).
[19] A. Nakagawa, S. Ishii, and T. Baba, Appl. Phys. Lett. **86**, 041112 (2005).
[20] D. K. Armani, T. J. Kippenberg, S. M. Spillane, and K. J. Vahala, Nature (London) **421**, 925 (2003).
[21] M. Cai, O. Painter, and K. J. Vahala, Phys. Rev. Lett. **85**, 74 (2000).
[22] S. M. Spillane, T. J. Kippenberg, O. J. Painter, and K. J. Vahala, Phys. Rev. Lett. **91**, 043902 (2003).
[23] V. S. Ilchenko, M. L. Gorodetsky, and S. P. Vyatchanin, Opt. Commun. **107**, 41 (1994).
[24] I. S. Grudinin and K. J. Vahala, Opt. Express**17**, 14 088 (2009).
[25] C. K. Law, Phys. Rev. A **51**, 2537 (1995).
[26] Y. R. Shen and N. Bloembergen, Phys. Rev. **137**, A1787 (1965).
[27] R. Y. Chiao, C. H. Townes, and B. P. Stoicheff, Phys. Rev. Lett. **12**, 592 (1964).
[28] T. J. Kippenberg, H. Rokhsari, T. Carmon, A. Scherer, and K. J. Vahala, Phys. Rev. Lett. **95**, 033901 (2005).
[29] V. B. Braginsky and F. Khalili, *Quantum Measurement* (Cambridge University Press, Cambridge, England, 1992).
[30] J. M. Dobrindt and T. J. Kippenberg, arXiv:0903.1013v1.
[31] M. Eichenfeld, J. Chan, R. M. Camacho, K. Vahala, and O. Painter, Nature (London) **462**, 08524 (2009).